

Variation of Fractional Electron Density Fluctuations near 0.1 AU from the Sun observed by Ulysses Dual-Frequency Ranging Measurements

Richard Woo and John W. Armstrong
Jet Propulsion Laboratory, California Institute of Technology, Pasadena, California

Michael K. Bird
Radioastronomisches Institut, Universität Bonn, Bonn, Germany

Martin Pätzold
Institut für Geophysik and Meteorologie, Universität zu Köln, Germany

Abstract

Although many properties of the ubiquitous electron density fluctuations near the source region of the solar wind have been obtained from radio scintillation and scattering observations, the relative strength of the fluctuations — characterized by fractional fluctuations $\delta n_e/n_e$ (δn_e is rms electron density fluctuation and n_e is the mean electron density) and providing clues about the nature and role of density fluctuations in the expansion of the solar wind --- has not been determined. The first measurements of $\delta n_e/n_e$ have been carried out inside $40 R_{\odot}$ using 1991 Ulysses dual-frequency S- and X-band (13 and 3.6 cm) ranging (time delay) measurements. In the frequency band of $\sim 6 \times 10^{-5} - 8 \times 10^{-4}$ Hz (periods of 20 min to 5 hr), $\delta n_e/n_e$ varies from a high of near 20% in the slow wind near the neutral line to a low of about 1 % in the fast wind far from the neutral line. For spatial wavenumber $K = 1.4 \times 10^{-6} \text{ km}^{-1}$ (5 hr period at 250 km s⁻¹), $\delta n_e/n_e$ is essentially independent of heliocentric distance over 0.03- 1.0 AU in the slow wind; it is a factor of 30 lower in the fast wind than in the slow wind inside 0.1 AU, but exhibits dramatic growth with heliocentric distance inside 0.3 AU. This latter result reinforces current views of the evolution of MHD turbulence and the association of Alfvén waves with high speed streams based on fields and particles measurements made beyond 0.3 AU. That regions of enhanced density fluctuations near or above the neutral line coincide with regions of enhanced density confirms previous conclusions that they are the interplanetary manifestation of the heliospheric current sheet and extensions of coronal

streamers. While the regions of enhanced density fluctuations lie within those of enhanced density, they have boundaries that are distinctly more abrupt, suggesting the separation of solar wind of different solar origin and wind speed.

Introduction

Radio scintillation and scattering measurements, conducted first with natural radio sources and later also with spacecraft radio signals, have revealed substantial electron density fluctuations in the inner heliosphere near the source region of the solar wind where *in situ* measurements have not yet been made. Much is known about the density fluctuations from such measurements, including the dependence of their fluctuation level δn_e on heliocentric distance, solar latitude, and solar cycle [Frickson, 1964; Bourgois and Colts, 1992], their anisotropy [Armstrong et al., 1990], and their spatial wavenumber spectrum [Woo and Armstrong, 1979; Colts et al., 1992]. A critical characteristic that has not been determined in the past is the level of relative or fractional density fluctuations $\delta n_e/n_e$ [Bourgois and Colts, 1992], which is important for understanding the nature and role of the near-Sun density fluctuations in the expansion of the solar wind [Marsch, 1991; Roberts and Goldstein, 1991]. Measuring relative density fluctuations has taken on added interest and significance with the recent discovery of large variations in δn_e in the vicinity of the Sun [Woo and Gazis, 1993; Woo et al., 1994]. Knowledge of relative density fluctuations also has relevance when density fluctuations inferred from radio scintillation and scattering measurements are used as a proxy for density [Newkirk, 1967; Houminer and Hewish, 1974; Ananthakrishnan et al., 1980; Tappin, 1986; Woo and Gazis, 1994].

Determination of fractional density fluctuations requires the measurement of absolute, electron density, which is provided by dual-frequency observations of time delay or ranging. Such measurements were conducted by the Ulysses Solar Corona Experiment [Bird et al., 1994] at wavelengths of 13.1 and 3.6 cm in August 1991 and form the basis of this study,

Observations and Results

Time delay, or ranging, measures path-integrated electron density or total electron content, but to a good approximation it is proportional to electron density n_e at the closest approach point of the radio path [Bird et al., 1994]. Thus, the ranging time series can be regarded equivalently as the time series of electron density, with the observed ranging scintillation representing the density fluctuations. As in the case of *in situ* plasma measurements, density fluctuations δn_e observed in this manner refer to fluctuations in the temporal (rather than spatial) domain.

Relevant portions of Fig. 4 of Bird et al. [1994] showing the contour map of coronal magnetic field strength at $2.5 R_{\odot}$ during the 1991 Ulysses radio measurements are reproduced in Figs. 1a and 2a; the map was provided by J. T. Hocksema, as adapted from Solar Geophysical data [Hocksema and Scherrer, 1986]. The crosses in Fig. 1a (dots in Fig. 2a) represent the closest approach points of the Ulysses radio path on the denoted days of year (DOY) during the ingress (egress) phase of superior conjunction, and hence indicate the corresponding approximate regions probed. Selected actual radio path segments near the closest approach points for a few days are also shown.

Using the 10-rev measurements of differential time delay, we have computed the mean values ($\Delta\tau$) and standard deviations ($\sigma\Delta\tau$) -- proportional to density and density fluctuations, respectively -- during the duration of each DSN tracking pass. Although the averaging periods were typically 5-10 hours long, there were a few cases with periods less than 2 hours. To remove the dependence on heliocentric distance, we have scaled the ingress and egress path-integrated measurements of time delay to 1 AU according to the radial dependencies of $R^{-1.54}$ and $R^{-1.42}$ determined by Bird et al. [1994], respectively. We have also scaled the standard deviations of time delay to 1 AU according to the radial dependence of $R^{-1.5}$, as has been observed in equivalent Doppler scintillation measurements near the Sun [Woo, 1978],

The time histories of normalized $\Delta\tau$ and $\sigma\Delta\tau$ in nanoseconds for ingress and egress are displayed in Figs. 1b and 2b, respectively. For convenience of comparison with the coronal field maps, the time axes have been reversed and displayed in such a manner that DOY lines up approximately with the corresponding crosses (dots) in Fig. 1a (Fig. 2a). Corresponding heliocentric distances are shown in Figs. 1d and 2d, indicating that the Ulysses measurements took place inside $40 R_{\odot}$.

As has been found in Bird et al. [1994], the density profiles in Figs. 1b and 2b exhibit peaks near the neutral line, and are the apparent extensions of coronal streamers that have also been observed by *in situ* plasma measurements surrounding sector boundaries at 1AU [Gosling et al., 1981; Huddleston et al., 1994]. While the profiles of δn_e for the frequency band of 5×10^{-5} -- 8×10^4 Hz in Figs. 1b and 2b follow the same general pattern as n_e , the variations of δn_e are distinctly more abrupt and significantly greater (larger than an order of magnitude for δn_e vs less than a factor of 2 for n_e). This is also demonstrated in plots of $\delta n_e/n_e$ in Figs. 1c and 2c --- obtained by dividing the standard deviations $\sigma\Delta\tau$ by the mean values $\Delta\tau$ of time delay -- showing variations of 1 -20% and an order of magnitude contrast (corresponding to two orders of magnitude contrast in spectral density levels) between fast (far from neutral line) and slow (near neutral line) solar wind. It should be emphasized that the contrasts here are of density fluctuations with the same fluctuation frequency, and it is more meaningful to compare fluctuations of the same spatial scale. Let us do this for fast (minimum $\delta n_e/n_e$) and slow (maximum $\delta n_e/n_e$) wind observed near the Sun by the Ulysses remote sensing radio measurements and beyond 0.3 AU by Helios *in situ* plasma measurements [Marsch and Tu, 1990]. Assuming a speed of 250 km/s for the slow wind near the Sun [Coles, 1993], the corresponding spatial wavenumber K ($K=2\pi f/v$, where f is fluctuation frequency and v is transverse solar wind speed) is $1.4 \times 10^{-6} \text{ km}^{-1}$ (corresponding to reduced wavenumber $k^* = 2.2 \times 10^{-7} \text{ km}^{-1}$ [Marsch and Tu, 1990]) for 5 hr fluctuations. For density fluctuations whose spatial wavenumber spectrum is Kolmogorov, δn_e (for fixed spatial wavenumber) $\sim v^{5/6}$ [Woo, 1978], Assuming that the

fast wind near the Sun is 500 km/s [Coles, 1993], observed values of $\delta n_e/n_e$ (fixed spatial wavenumber) for the fast wind would, therefore, have to be reduced by a factor of $(500/250)^{5/6} = 1.78$. We combine estimates of $\delta n_e/n_e$ beyond 0.3 AU deduced from the Helios spatial wavenumber spectra shown in Fig. 6 of Marsch and Tu [1990] with the near-Sun scintillation results in Fig. 3. The Ulysses data points for the slow wind represent the three highest values of $\delta n_e/n_e$ observed (DOY 228.11, 234.88 and 240.85), and the data points for the fast wind the six lowest values of $\delta n_e/n_e$ (DOY 221.89, 224.83, 226.89, 236.84, 237.82 and 248.11). The dashed curves -- quadratic in the case of the fast wind and constant in the case of the slow wind --- are intended to guide the eye. While $\delta n_e/n_e$ of the slow wind shows little dependence on heliocentric distance, $\delta n_e/n_e$ of the fast wind inside 0.1 AU is significantly lower than that of the slow wind (as high as a factor of 30 in amplitude and nearly 3 orders of magnitude in spectra density level) and exhibits dramatic growth with heliocentric distance inside 0.3 AU. We have also fit a power-law to the fast wind results and find that the amplitude is roughly proportional to solar distance. It should be pointed out that although mean densities were computed differently --- over a period of a day in the case of the Helios plasma measurements and over the length of a track (typically about 5 hrs) in the case of the Ulysses ranging measurements --- we expect this to have little effect on the conclusions of this paper.

Finally, we have also plotted normalized $\Delta\tau$ in Figs. 1c and 2c showing that normalized $\Delta\tau$, and hence normalized n_e , approximately tracks variations in $\delta n_e/n_e$. This is apparently a consequence of the fact that n_e varies more slowly than δn_e , and is highly significant, because it means that it is possible to obtain information on variations in fractional density fluctuations even when only measurements of density fluctuations are available, such as in the case of Doppler scintillation [Woo and Gazis, 1993].

Conclusions and Discussion

Using ranging measurements of absolute electron density, the first investigation of $\delta n_e/n_e$ in the frequency band of $6 \times 10^{-5} - 8 \times 10^{-4}$ Hz inside 40 R. shows that it varies

from 1 to 20%. As with density fluctuations in a higher frequency band (3×10^{-3} - 5×10^{-2} Hz) studied earlier [Woo and Gazis, 1993], density fluctuations in the lower frequency band are highest near the neutral line where the solar wind is slow, and lowest far from the neutral line where the solar wind is fast. These results reinforce the fact that the density spectrum near the Sun depends strongly on proximity to the neutral line [Woo et al., 1994] and cannot be represented by a single spectrum [Woo and Arretong, 1979; Coles et al., 1991]. The similarity between Ulysses ranging measurements of low-frequency fluctuations and Pioneer Venus Doppler scintillation measurements of high-frequency fluctuations is also consistent with the broadband nature of increase in electron density spectrum observed by Voyager [Coles et al., 1991] during the passage of 'transients,' some of which represent the extensions of coronal streamers.

For spatial wavenumber $K = 1.4 \times 10^{-6} \text{ km}^{-1}$, $\delta n_e/n_e$ is essentially independent of heliocentric distance in the slow wind, while in the case of the fast wind, it is a factor of 30 lower than that of the slow wind inside 0.1 AU, and exhibits dramatic growth with heliocentric distance inside 0.3 AU. This latter result reinforces current views of the evolution of MHD turbulence with solar wind expansion and the association of Alfvén waves with high speed streams based on fields and particles measurements made beyond 0.3 AU [Marsch and Tu, 1990; Roberts and Goldstein, 1991; Bavassano, 1994]. The remarkably low density fluctuations associated with the fast wind also strengthens the argument for the presence of magnetic field fluctuations and Alfvén waves in high speed streams deduced from Faraday rotation fluctuations observed near the Sun [Hollweg et al., 1982].

That regions of enhanced density fluctuations near or above the neutral line coincide with regions of enhanced density confirms previous conclusions that they are the interplanetary manifestation of the heliospheric current sheet and extensions of coronal streamers [Woo et al., 1994]. While the regions of enhanced density fluctuations lie within those of enhanced density, they have boundaries that are distinctly more abrupt, suggesting

the separation of solar wind of different solar origin and wind speed. *In situ* measurements by ISEE-3 show that the abrupt boundary west of the sector boundary survives to at least 1 AU [Huddleston et al., 1994]. Since n_e varies more slowly than δn_e , variations in δn_e reflect approximately those of $\delta n_e/n_e$, thus making it possible to obtain information on variations in relative density fluctuations even when only measurements of density fluctuations are available. That variations in δn_e near the Sun are more abrupt and prominent than variations in mean electron density enhances the value of measurements based on sensing density fluctuations for observing and investigating the interplanetary manifestation of solar phenomena. The large contrasts in $\delta n_e/n_e$ indicate that the use of density fluctuations as a proxy for density, at least for periods longer than ten minutes, can be misleading especially near the Sun. It is clear that further studies including comparisons with solar observations will lead to a better understanding of the wealth of dynamic interplanetary phenomena observed in scintillation measurements near the Sun.

Acknowledgments. It is a pleasure to acknowledge the outstanding support received from the Ulysses Project, the NASA Deep Space Network, and the Radio Science Support Team. We are especially grateful to C. Chang and J. Karl (Universität zu Köln) for programming and data processing, and to S. Asmar, A. Devcereaux, P. Eshe, R. Herrera, "1". Horton and D. Morabito for support. continuous or near-continuous tracking of Ulysses by the DSN was key to the results of this study, and we would like to thank J. Brenkle for his efforts in arranging it. This paper presents results of a research project partially funded by the Deutsche Agentur für Raumfahrtangelegenheiten (DARA) GmbH under the contracts 50 ON 9104 and 50 QM 5411, and describes research carried out at the Jet Propulsion Laboratory, California Institute of Technology, under a contract with NASA. The responsibility for the contents of this publication is assumed by the authors.

REFERENCES

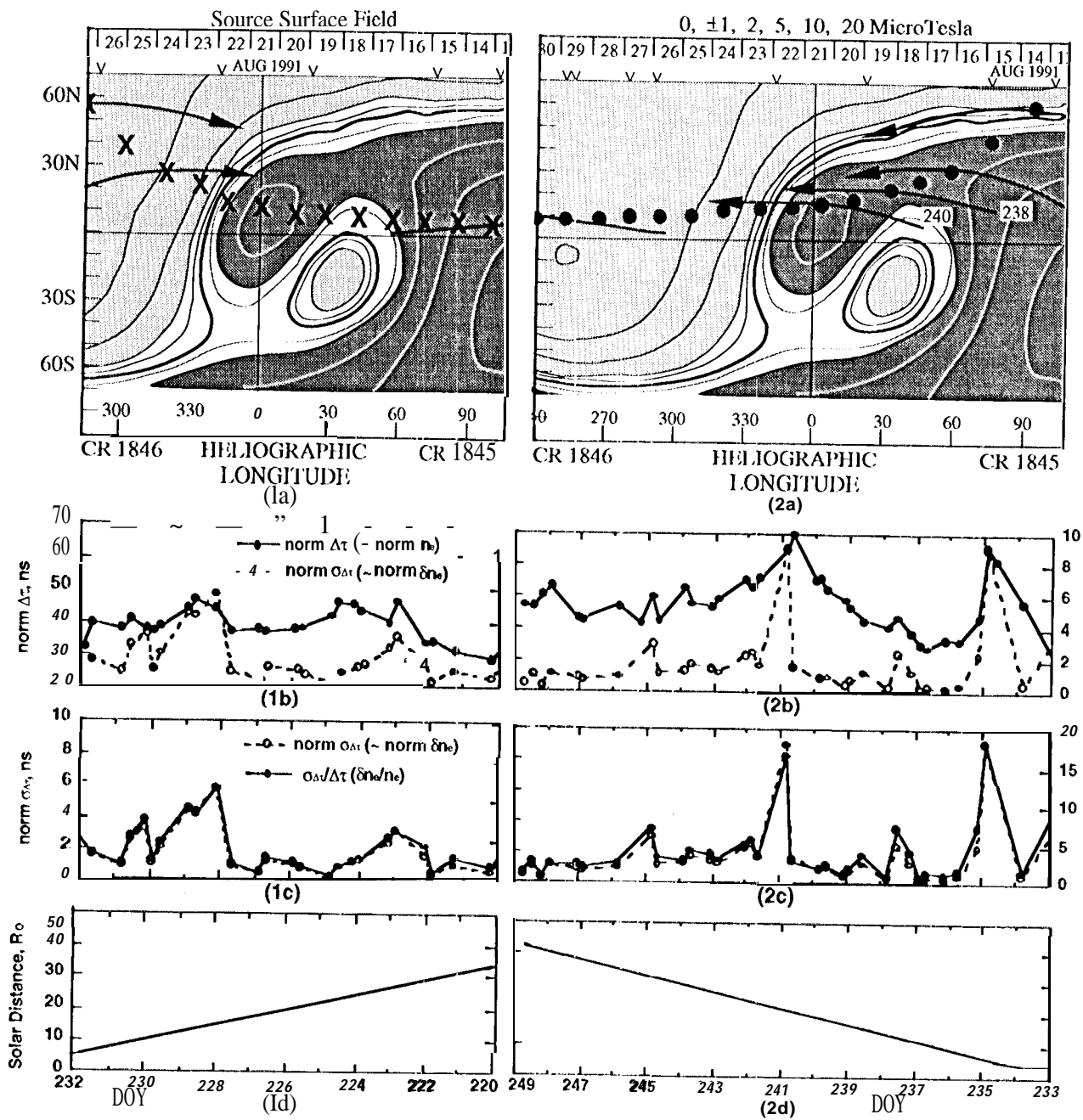
- Ananthakrishnan, S., W.A.Coles and J.J. Kaufman, Microturbulence in solar wind streams, *J.Geophys.Res.*, *85*, 6025-6030, 1980.
- Armstrong, J.W., W.A.Coles, M. Kojima, and B.J.Rickett, Observations of field-aligned density fluctuations in the inner solar wind, *Astrophys.J.*, *3.58*, 685-692, 1990.
- Bavassano, B., Recent observations of MHD fluctuations in the solar wind, *Ann. Geophys.*, *12*, 97, 1994.
- Bird, M. K., 11. Volland, M, Pätzold, P. Eidenhofer, S.W. Asmar, and J. F. Brenkle, The coronal electron density distribution determined from dual-frequency ranging measurements during the 1991 solar conjunction of the Ulysses spacecraft. *Astrophys. J.*, *426*, 373-381, 1994.
- Bourgois, G., and W.A.Coles, Solar cycle changes in the turbulence level of the polar stream near the Sun, in *Solar Wind Seven*, eds. F. Marsch and R. Schwenn, pp. 155-158, Pergamon Press, Oxford, 1992.
- Coles, W. A., Scintillation in the solar wind (IPS), in *Wave Propagation in Random Media (Scintillation)*, eds. V. Tatarskii, A. Ishimaru and V. Zavorotny, 156-168, SPIE, Bellingham, WA, 1993.
- Coles, W. A., Liu, W., J.K. Harmon, and C.L. Marlin, The solar wind density spectrum near the Sun: Results from Voyager radio measurements, *J.Geophys.Res.*, *96*, 1745-1755, 1991.
- Frickson, W.C., The radio-wave scattering properties of the solar corona, *Astrophys. J.*, *139*, 1290-1311, 1964.
- Gosling, J.'J.', G. Borrini, J.R. Asbridge, S.J. Bame, W. C. Feldman, and R.T. Hansen, Coronal streamers in the solar wind at 1AU, *J.Geophys.Res.*, *86*, 5438-5448, 1981.
- Hoeksema, J.'J.', and P.'H. Scherrer, The solar magnetic field -1976 through 1985, *Rep. UAG-94*, World Data Cent. A for Sol. Terr. Phys., Boulder, Colo., 1986.

- Hollweg, J. V., M.K. Bird, H. Volland, P. Edenhofer, C.T. Stelzried, and H. Scidel, *J. Geophys. Res.*, 87, 1-8, 1982.
- Houminer, Z., and A. Hewish, Correlation of interplanetary scintillation and spacecraft plasma density measurements, *Planet. Space Sci.*, 20, 1041-1042, 1974.
- Huddleston, D.E., R. Woo, and M. Neugebauer, Density fluctuations in different solar wind flows at 1AU, *J. Geophys. Res.*, in preparation.
- Marsch, E., MHD turbulence in the solar wind, in *Physics of the inner Heliosphere II*, eds. R. Schwenn and E. Marsch, pp. 159-241, Springer-Verlag, Berlin, 1991.
- Marsch, E., and C.-Y. Tu, Spectral and spatial evolution of compressible turbulence in the inner solar wind, *J. Geophys. Res.*, 95, 11945-11956, 1990.
- Newkirk, G., Structure of the solar corona, *Rev. Astron. Astrophys.*, 5, 213-263, 1967.
- Roberts, D. A., and M.J. Goldstein, Turbulence and waves in the solar wind, *Rev. Geophys.*, 29, 932-943, 1991
- Tappin, S. J., interplanetary scintillation and plasma density, *Planet. Space Sci.*, 34, 93-97, 1986.
- Woo, R., Radial dependence of solar wind properties deduced from Helios 1/2 and Pioneer 10/11 radio scattering observations, *Astrophys. J.*, 219, 727-739, 1978.
- Woo, R., and J.W. Armstrong, Spacecraft radio scattering observations of the power spectrum of electron density fluctuations in the solar wind, *J. Geophys. Res.*, 84, 7288-7296, 1979.
- Woo, R., and P.R. Gazis, Large-scale solar-wind structure near the Sun detected by Doppler scintillation, *Nature*, 366, 543-545, 1993.
- Woo, R., and P.R. Gazis, Mass flux in the ecliptic plane and near the Sun deduced from Doppler scintillation, *Geophys. Res. Letters*, 21, 1101-1104, 1994.
- Woo, R., J.W. Armstrong, and P.R. Gazis, Doppler scintillation measurements of the heliospheric current sheet and coronal streamers close to the sun, *Space Sci. Rev.*, in press, 1994.

FIGURE CAPTIONS

Figs. 1 and 2. Measurements during ingress (Fig. 1) and egress (Fig. 2): (a) Closest approach points (crosses in Fig. 1, dots in Fig. 2) of radio path projected onto contour map of coronal magnetic field strength at $2.5 R_{\odot}$, (b) normalized time delay $\Delta\tau$ (- normalized n_e) and normalized time delay scintillation $\sigma\Delta\tau$ (\sim normalized δn_e), (d) normalized $\sigma\Delta\tau$ (- normalized δn_e) and $\sigma\Delta\tau/\Delta\tau$ ($\delta n_e/n_e$), and (c) radial distance in solar radii.

Fig. 3. Fractional density fluctuations $\delta n_e/n_e$ for spatial wavenumber $K = 1.4 \times 10^{-6} \text{ km}^{-1}$ (reduced wavenumber $2.2 \times 10^{-7} \text{ km}^{-1}$). Solid and hollow circles are Ulysses ranging measurements; solid and hollow triangles are Helios *in situ* plasma measurements. Solid points are for fast wind and hollow points for slow wind. Dashed curve for the fast wind (far from the neutral line) is a quadratic fit to the data, while dashed curve for the slow wind (near the neutral line) represents a constant.



Figs 1 & 2

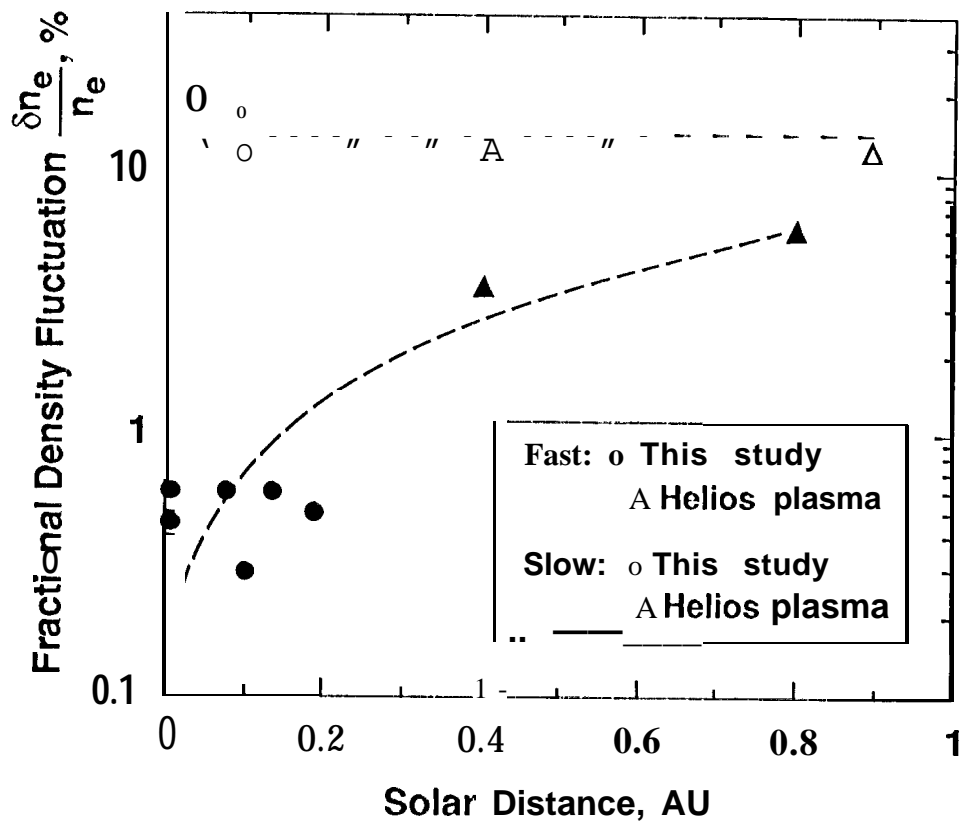


Fig. 3